Available online at www.sciencedirect.com
SCIENCE DIRECT
Journal of the European Ceramic Society 26 (2006) 1363–1370
www.elsevier.com/locate/jeurceramsoc

Influence of the precursors on the formation and properties of the $Fe_xCr_{2-x}O_3$ solid solution

Raquel Muñoz, Mónica Martos, Catalin M. Rotaru, Héctor Beltrán, Eloisa Cordoncillo, Purificación Escribano *

Departamento de Química Inorgánica y Orgánica, Universitat Jaume I, Campus Riu Sec, 12071 Castellón de la Plana, Spain

Received 22 September 2004; received in revised form 1 February 2005; accepted 12 February 2005
Available online 31 March 2005

Abstract

A black pigment was synthesised based on $Fe_xCr_{2-x}O_3$ stoichiometry, by studying the compositions with $x = 0.15$, 0.20, 0.50, 1.00, 1.20, 1.30, 1.50, 1.80 and 1.85 and using industrial grade reagents as raw materials. The resulting products were compared with a pigment made using chemically pure (CP grade) reagents in order to establish the most appropriate reagents for achieving minimum Cr(VI) segregation during the pigment washing stage, and comparable chromatic qualities of a standard industrial pigment. X-ray diffraction (XRD) indicates a solid solution formation based on the haematite structure; however, X-ray photoelectron spectroscopy (XPS) and Mössbauer analysis indicate the presence of a phase containing Fe(II) undetected by XRD. A smaller Cr(VI) content was found in the washing liquids when industrial grade reagents were used, but the resulting chromatic quality was poorer than that obtained for the same composition when made with CP grade raw materials.

Keyword: $(Fe,Cr)_2O_3$; Pigments; Raw materials

1. Introduction

With few exceptions, inorganic pigments are oxides, sulphides, oxide hydroxides, silicates, sulphates or carbonates and can consist of single-component particles (e.g., red iron, α-Fe_2O_3) with well-defined crystal structures or mixed pigments made up of non-uniform or multicomponent particles and, in general, they contain transition metal ions.[1]

Ceramic pigment research is directed towards achieving a greater understanding of pigment-forming systems and finding useful new pigments for different applications in glazes, porcelain enamels, paints and plastics.

Ceramic pigment synthesis by the ceramic method, as in any solid-state reaction, entails the drawback that the reaction mechanism is kinetically controlled by slow atomic diffusion processes in the crystal lattice, which essentially depend on the number of ionic defects in the lattice, of their mobility and of the thermodynamic force governing the process. These problems require ceramic pigment synthesis reactions to take place at high temperatures with long reaction times, which affect the economic costs of the process and may alter end product stoichiometry as a result of volatilisation of the volatile components during calcination. Volatilisation losses, together with the soluble products that may be removed in the washing stages, are important sources of pollution in the sector and, given current regulatory restrictions, make it increasingly necessary to study systems that contain potential pollutants with a view to substituting and/or reducing these.

As a result, the focus of research in the field of ceramic pigments tends to be determined by socio-economic, sanitary or environmental factors or the enhancement of the pigmenting power of currently known structures.

Among the pigmenting systems that pose the greatest risks, there are those that contain ions of the first transition series, such as chromium, cobalt, nickel, etc., as the d-block metals show an extremely wide range of both redox behaviour

* Corresponding author.
E-mail address: escriban@qio.uji.es (P. Escribano).

0955-2219/$ – see front matter © 2005 Elsevier Ltd. All rights reserved.
doi:10.1016/j.jeurceramsoc.2005.02.008

and complex formation. These properties underlie their catalytic role in enzyme action.[2]

The light absorption coefficient of black pigments determines their optical quality. Their colour intensity and hiding power depend on the particle size and particle size distribution. The most important black pigments are carbon blacks, iron oxides, and mixed metal oxides. Due to the high temperatures used in the ceramic industry, carbon black pigments are not suitable as ceramic pigments, which is why black ceramic pigments are based on iron oxides and mixed metal oxides, and particularly on the latter.

In fact, black ceramic pigments are formed by mixing several divalent and trivalent oxides which, after firing, form the most common spinel structure. The divalent ions may be iron, cobalt, manganese, nickel or copper. The trivalent ions may be iron, chromium, manganese or aluminium.[3] The spinel lattice not only possesses good thermal and chemical stability, but also a high refractive index, which is important for good optical pigment properties and, by charge transfer, can generate a black colour by strong absorption of the whole spectrum.

The traditional way to obtain an intense black colour in a ceramic glaze is to disperse a quantity of cobalt–iron–chromite[4] material, in some cases also containing Ni(II), in a glaze. Cobalt-free iron–chromium pigments have been the focus of renewed interest in recent years because of the increase in price of cobalt-bearing black pigments and their pollution problems.[5] There is, therefore, a need for an intense black pigment free of cobalt oxide and suitable for use in ceramic glazes.[4] A patent of the synthesis of this cobalt-free pigment can be found in the literature.[6]

Cr-doped structures have been widely studied as ceramic pigments.[7–9] Chromium is necessary to obtain a black pigment. Depending on synthesis conditions, it can be found in different states of oxidation (II–VI) and these generate different properties, stability and coloration. This difficulty in understanding the colouring mechanism involved and the few related studies found in the literature have led to undertaking this study on chromium-containing pigmenting systems, trying to keep the Cr(III) ion from oxidising to Cr(VI) because of its negative environmental impact, as it is segregated in the washing liquids.[5]

Cr(VI) is taken into the body through the respiratory system (the handling of Cr(VI) precursors by workers), water or food (due to irrigation with polluted water) and can cause acute gastroenteritis, allergic dermatitis, chronic conjunctivitis, rhinopharyngitis and lung cancer.

Thus, a factor to be kept in mind is the handling of Cr(VI) precursors. The National Institute of Occupational Health and Safety recommended that the chromium (VI) compound quantity handled should not exceed 1 mg/m^3 during 10 working hours a day.[10–14] Another problem associated with the use of Cr(VI) is the fact that the ceramic pigments have to be washed before application in a glaze, and the content of water-soluble or acid-soluble chromium is becoming important from a toxicological and ecological point of view.

Nickel and its compounds also represent a risk factor as they are potential carcinogens in human beings and animals. In plants they have a phytotoxic action when present in high concentrations.

Owing to the great number of oxides present in the structure, in practice it is difficult to reproduce a black colour of high optical quality. This fact, together with the use of transition metals, considered toxic according to Environmental Protection Agency (EPA) guidelines, makes it of interest to conduct an in-depth study of these pigments in order to attempt to reduce the content and number of toxic elements, and to try to replace these with f-block elements, as the f-block metals (lanthanides and actinides), although showing a wide range of redox behaviour and complex formation, are usually biologically unimportant with the exception of some of the actinide group, which may be significant pollutants.

In the ceramic industry, a ceramic pigment is used that contains Cr_2O_3, MnO, Fe_2O_3, NiO and Pr_6O_{11} (used as STD reference in this study). In addition to a good understanding of the parameters that control the synthesis of this black pigment, thorough raw materials control, reduction of energy costs and, specifically, modification of the processes are required to attempt to achieve zero emissions and waste. This is moreover necessary for the product to meet growing social demands with regard to safety, sustainability and minimal environmental impact.

Given the complexity of the system owing to the number of components and problems relating to the use of highly pollutant raw materials, it has been considered useful to study binary compositions with oxides that appear in their formulation and which, according to the DCMA[15] classification, will exhibit a black coloration. The present study therefore addresses the synthesis of the black pigment referenced 3-05-3 Chromium green–black haematite. This will subsequently be followed by a study of other binary combinations which, together with the pigment oxides used in industry, develop the black colour.

Structurally, the iron and chromium black pigment is a solid solution of Fe_2O_3 and Cr_2O_3. In the phase diagram of this system,[16] these oxides can be observed to generate a complete corundum solid solution for all the range of compositions up to ~1400 °C. Above this temperature, Fe_2O_3 is reduced to FeO and an $Fe(Fe,Cr)_2O_4$ brown spinel can also form.

The Fe_2O_3 and Cr_2O_3 solid solution is a substitutional type in which Fe^{3+} and Cr^{3+} ions are distributed at random over the octahedral sites in the corundum structure. The solid solution may be formulated as $Fe_xCr_{2-x}O_3$ ($0 \leq x \leq 2$). The raw materials used in synthesis explain the black colour of this pigment. The intense red colour of Fe_2O_3 can be attributed to an $O^{2-} \rightarrow Fe^{3+}$ charge transfer mechanism. The green colour of Cr_2O_3 is originated by d–d transitions in Cr^{3+}. The two mechanisms produce an overlapping absorption that covers the visible spectrum with a resulting black pigment.

The aim of this research is to study the influence of the mixing ratio of Fe_2O_3 and Cr_2O_3 in the black coloration of

this pigment and also to optimise its synthesis in order to reduce the amount of Cr(VI) in the washing liquids (crucial operation in the manufacture of this pigment) without decreasing its pigmenting properties.

2. Experimental

In accordance with the traditional ceramic pigment synthesis route, several compositions based on $Fe_xCr_{2-x}O_3$ stoichiometry ($x = 0.15$, 0.20, 0.50, 1.00, 1.20, 1.30, 1.50, 1.80 and 1.85) have been prepared. The different mixtures were refined and homogenised by wet milling in acetone in a laboratory planetary ball mill for 20 min. After drying, the samples were fired in a Nabertherm electric furnace at a heating rate of 10 °C/min at 1100, 1200 and 1300 °C and held at each final temperature for 2 h. To refine and homogenise the particle size after calcining, the resulting products were ground in an agate mill with acetone, followed by sieving at 50 μm. All the measurements in this study were performed on the sieved samples.

In a first stage, the different samples used in this study were synthesised from ferric oxide and chromic oxide of the quality commonly used in the ceramic colorant industry, with a view to conducting the experiments under conditions similar to those found on an industrial scale. Table 1 details the chemical composition of the two oxides, determined by X-ray fluorescence (XRF) measurements using a SIEMENS SRS 3000 wavelength dispersive XRF spectrophotometer.

Phase analysis of the fired samples has been performed by X-ray powder diffraction (XRD) with a SIEMENS D5000 diffractometer with Cu Kα radiation. Data have been collected by step-scanning from 20 to 70 °2θ with a step size of 0.05 °2θ and 5 s counting time at each step at room temperature. The goniometer was controlled by the "SIEMENS DIFFRACT plus" software, which also determined diffraction peak positions and intensities. The instrument was calibrated using an external Si standard. The spectra have been compared with those obtained for pure Cr_2O_3 and Fe_2O_3.

In order to determine the best temperature for obtaining a black pigment with high optical properties, a colorimetric study was performed and the $L^*a^*b^*$ data have been compared with those of a black pigment used in the ceramic industry, referenced STD. CIELAB colour parameters were determined at room temperature with a VARIAN UV/visible spectrophotometer (Model CARY 500 SCAN) and a coupled analytical software for colour measurements. The data were registered from 380 to 700 nm using a PTFE blank as reflecting standard. CIELAB colour parameter measurements were conducted using a D65 standard illuminant. Colorimetry serves to characterise a colour and allow identification. In this system, L^* is the lightness axis [black (0) to white (100)], a^* is the green (<0) to red (>0), and b^* is the blue (<0) to yellow (>0) axis.[17,18]

Table 1
Chemical composition of the industrial grade Cr_2O_3 and Fe_2O_3

Cr_2O_3 (industrial grade)			
SiO_2	P_2O_5	CaO	Cr_2O_3
0.0969%	0.5110%	0.0969%	99.3000%
Fe_2O_3 (industrial grade)			
S		TiO_2	Fe_2O_3
0.4445%		0.1000%	99.4554%

After obtaining the composition and temperature at which the pigment exhibited the best optical properties, we studied the Cr(VI) content in the washing liquids by a colorimetric method recommended by the EPA.[19] Thus, 0.3 g fired sample was subjected to successive washings with hot 0.3 M HNO_3 until obtaining 50 mL solution. Measurements were conducted on the spectrophotometer used for CIELAB measurements at 540 nm.

After establishing the composition and temperature at which the black pigment with the best optical characteristics developed, we proceeded to synthesise this under the same conditions, however using chemically pure (CP) grade reagents: Cr_2O_3 (J. Baker, 99.3%, impurities specified on the container: Max.: NH_4^+ 0.01%; Cl^- 0.02%; Fe 0.05% and SO_4^{2-} 0.7%). The sample was analysed by XRD, colorimetric measurements were made on the powdered samples and the Cr(VI) content in the washing liquids was determined.

To determine the particle size of the industrial grade and CP grade raw materials, these underwent the same grinding process, prior to calcination, used in mixing and homogenising the compositions being studied. Particle size of the ground raw materials was measured in a Coulter LS230 with micro volume module. The particle-size range which can be determined by this instrument lies between 0.4 and 2000 μm.

With a view to verifying the oxidation state of iron in the two samples selected, based on the data obtained by the various characterisation techniques, and the formation of the $Fe_xCr_{2-x}O_3$ solid solution, Mössbauer spectra were recorded using a conventional Mössbauer spectrometer with a ^{57}Co/Rh source where velocity calibration was done using a high-purity natural iron foil of 25 μm thickness, and the Mössbauer parameters are given relative to this standard at room temperature. Mössbauer data were fitted using the NORMOS program.

To confirm the results obtained by Mössbauer spectroscopy, X-ray photoelectron spectroscopy (XPS) spectra were obtained with a VG-Escalab 210 spectrometer operating in the fixed analyser transmission mode with a pass energy of 50 eV, and using a non-monochromated Al Kα ($h\nu = 1486.6$ eV) X-ray radiation. The pressure in the analyser chamber was kept at 10^{-9} mbar during spectra acquisition. Prior to XPS measurements the samples were degassed at room temperature at 10^{-6} mbar during night.

The binding energy was regulated by setting the C1s transition at 284.5 eV. The data analysis procedure involved smoothing, background subtraction and curve fitting using mixed Gaussian–Lorentzian functions by a least-squares

method. Atomic ratios of elements were calculated from the relative peak areas of the respective core level lines using the Wagner sensitivity factors.[20]

3. Results and discussion

The evolution of the crystalline phases in the different compositions studied after calcination at 1100, 1200 and 1300 °C with a 2-h soaking time at peak temperature was analysed by XRD. The diffractograms indicate the presence of $Fe_xCr_{2-x}O_3$ solid solution as the sole phase at the three test temperatures.

As an example, Fig. 1 depicts the diffractograms for some of the compositions synthesised after firing at 1200 °C/2 h, together with those of the Fe_2O_3 and Cr_2O_3 raw materials for comparison. It can be observed that when x increases (Cr_2O_3 decreases) the 2θ position of the peaks decreases and shifts to the Fe_2O_3 2θ position. The results are in good agreement with the theory because the d-spacing between the reticular planes in the Fe_2O_3 structure is larger than the d-spacing between the reticular planes in the Cr_2O_3 structure. According to Shannon and Prewitt data,[21] the atomic radii for Fe(III) (in a high spin situation) and Cr(III), both in octahedral coordination, are 78.5 and 75.5 pm, respectively: $d(Fe_2O_3) > d(Cr_2O_3)$ and taking into account Bragg's Law, $\theta(Fe_2O_3) < \theta(Cr_2O_3)$. The XRD spectra indicate that a solid solution is formed after the reaction of Fe_2O_3 and Cr_2O_3 at the test temperatures, because the corresponding d-spacing between the reticular planes changes according to the degree of substitution.

Fig. 2 displays the colorimetric study performed on the powdered samples. The figure shows that sample $Fe_{1.3}Cr_{0.7}O_3$ fired at 1200 °C with a 2-h soaking time exhibits the best optical properties compared with those of the standard industrial pigment (STD) ($L^* = 15.8300$, $a^* = 0.8959$ and $b^* = -0.4893$), because it displays a low L^* value (less clarity), while a^* and b^* values are also the lowest.

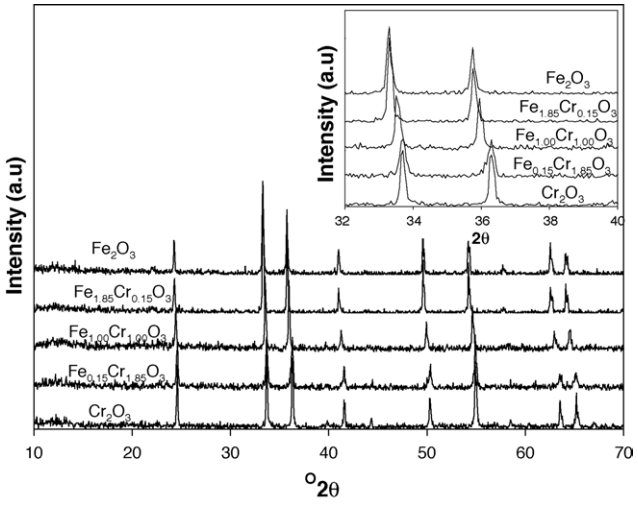

Fig. 1. XRD for some of the compositions fired at 1200 °C/2 h.

Analysis of the Cr(VI) content in the washing liquids of all the compositions after firing at the three test temperatures indicates that the smallest quantity is obtained for $x = 1.3$ at the three firing temperatures as shown in Fig. 3.

In view of the results obtained by XRD, colorimetry and analysis of Cr(VI) in the $Fe_{1.3}Cr_{0.7}O_3$ sample synthe-

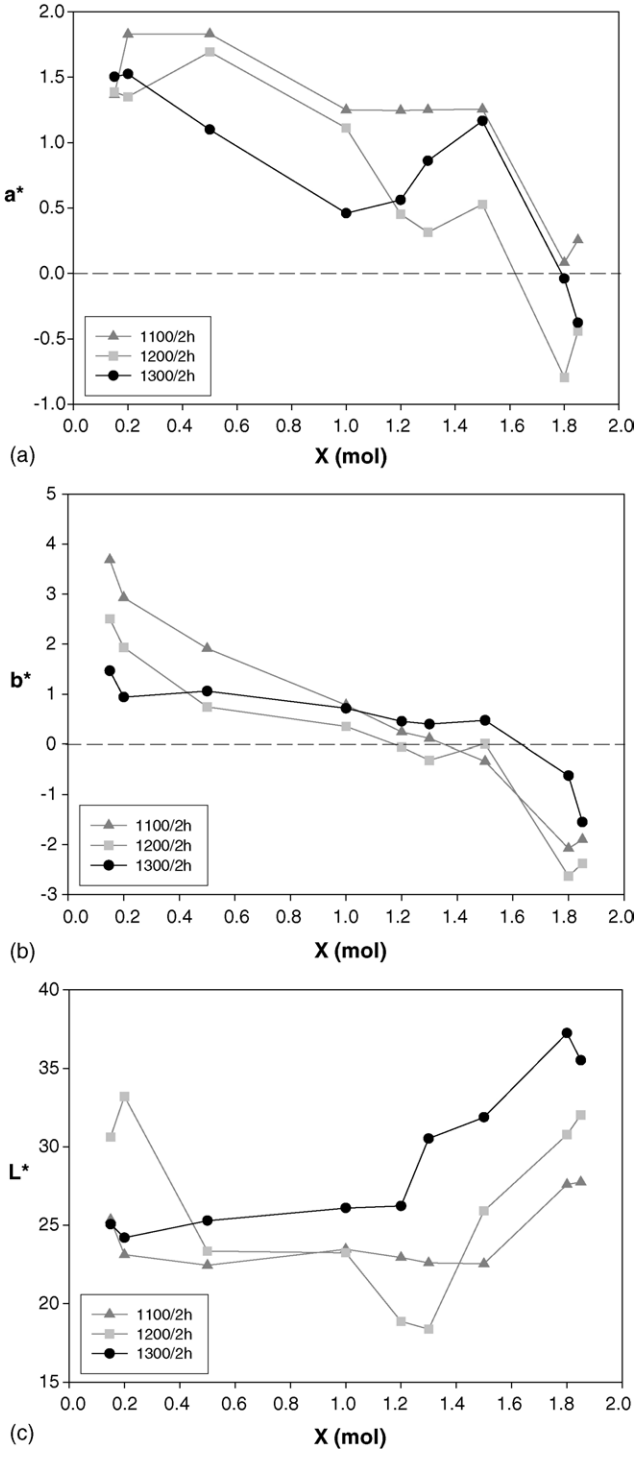

Fig. 2. Colorimetric coordinates in the fired samples: (a) a^*, (b) b^* and (c) L^*.

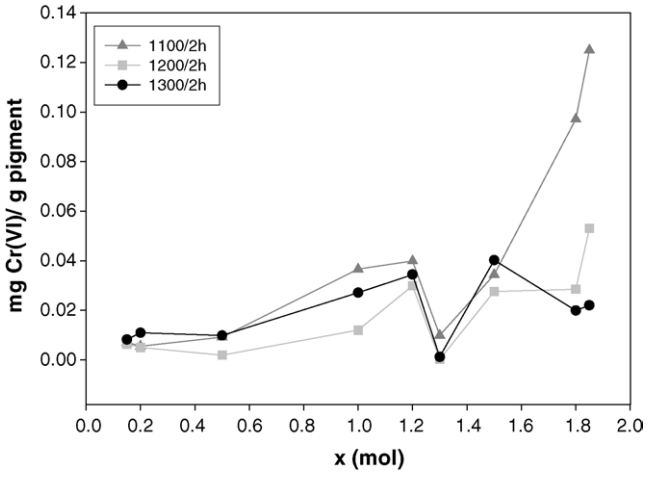

Fig. 3. Cr(VI) content in the washing liquids of all the compositions after firing at 1100, 1200 and 1300 °C/2 h.

Table 2
Chromatic coordinates of samples $Fe_{1.3}Cr_{0.7}O_3$ (I) and $Fe_{1.3}Cr_{0.7}O_3$ (L) calcined at 1200 °C/2 h

Samples	L^*	a^*	b^*
$Fe_{1.3}Cr_{0.7}O_3$ (I)	18.3854	0.3143	−0.3133
$Fe_{1.3}Cr_{0.7}O_3$ (L)	15.1466	0.2198	0.4917
STD	15.8300	0.8959	−0.4893

sised with industrial grade raw materials and calcined at 1200 °C/2 h, this temperature and soaking time were selected as a reference and this sample was then synthesised with CP grade raw materials; these samples are respectively referenced hereafter $Fe_{1.3}Cr_{0.7}O_3$ (I) and $Fe_{1.3}Cr_{0.7}O_3$ (L). The results obtained, both with regard to the chromatic coordinates and Cr(VI) content in the washing liquids are respectively shown in Tables 2 and 3.

The values of $L^*a^*b^*$ indicate an improvement in the optical qualities of the pigment in comparison with those obtained using industrial grade reagents, though a larger quantity of Cr(VI) is segregated in the washing liquids.

With a view to establishing whether the end stoichiometry matched the nominal starting stoichiometry, the quantity of Fe and Cr in samples $Fe_{1.3}Cr_{0.7}O_4$ (I) and $Fe_{1.3}Cr_{0.7}O_4$ (L) after calcination at 1200 °C/2 h was analysed by XRF. The analysis data show an Fe_2O_3 and Cr_2O_3 content of 64.80% and 34.60% respectively for sample (I), and 65.40% and 34.30% for sample (L), so that the ratio of Fe/Cr in (I) is 1.78 and in (L) 1.86. Comparison of these ratios with the initial ratio of 1.86 thus indicates that the quantity of Cr_2O_3 lost during calcination is slightly higher in the sample prepared with chemically pure reagents.

Table 3
Cr(VI) content in the washing liquids for samples $Fe_{1.3}Cr_{0.7}O_3$ (I) and $Fe_{1.3}Cr_{0.7}O_3$ (L) calcined at 1200 °C/2 h

Samples	mg Cr(VI)/g pigment
$Fe_{1.3}Cr_{0.7}O_3$ (I)	0.00018
$Fe_{1.3}Cr_{0.7}O_3$ (L)	0.02880

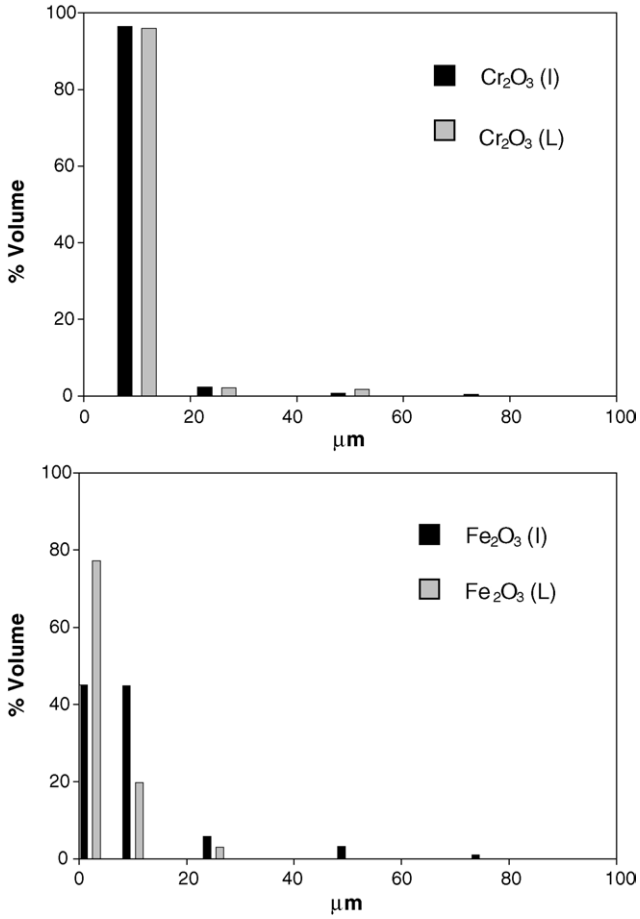

Fig. 4. Particle size of the industrial grade and CP grade raw materials Cr_2O_3 and Fe_2O_3.

Given the differences found with respect to the chromatic coordinates and Cr(VI) content in the washing liquids and taking into account that the reactivity of a mixture of solids is influenced by the contact area between the reacting solids and hence their surface areas, the particle size of both the industrial grade and CP grade raw materials Cr_2O_3 and Fe_2O_3 was measured. These results are shown in Fig. 4.

The figure shows that the two chromium oxides have a similar particle size, while there is a greater difference in size in the two iron oxides. Thus, ∼45% of the Fe_2O_3 (I) particles is similar in size to the Cr_2O_3 (I) particles, while 45% exhibits a much smaller size. In the case of Fe_2O_3 (L) only ∼20% of the particles is similar in size to the Cr_2O_3 (L) particles, and ∼78% is much smaller.

Particle size is known to be an important parameter, which strongly influences powder characteristics. If the mechanism proposed by Escardino et al.[22] is assumed for this system, a greater difference in sizes between the reacting oxide particles (the case of the sample prepared with CP grade raw materials) will affect the thickness of the Cr_2O_3 gaseous phase that is deposited on the Fe_2O_3 as well as the quantity of Cr(III)

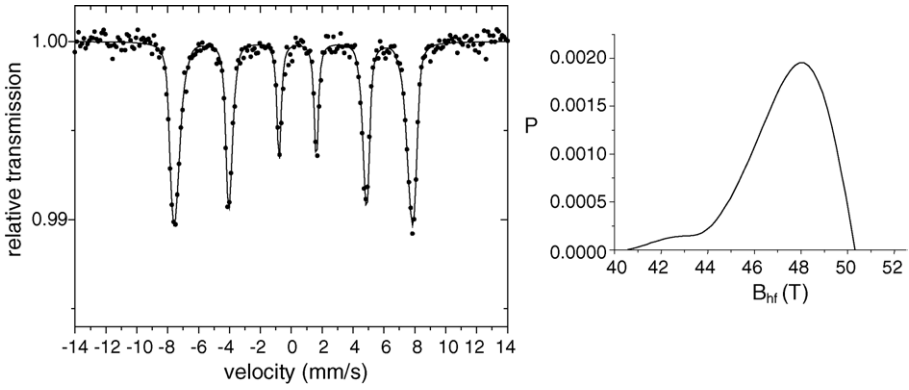

Fig. 5. Mössbauer spectra and hyperfine field distribution for $Fe_{1..3}Cr_{0.7}O_3$ (I).

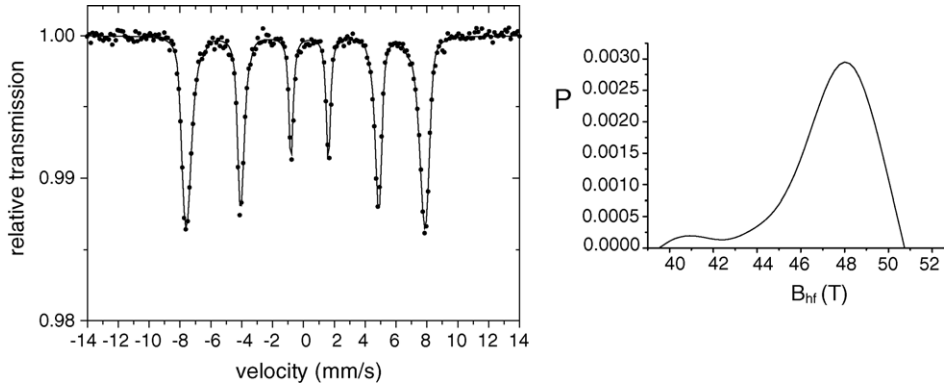

Fig. 6. Mössbauer spectra and hyperfine field distribution for $Fe_{1.3}Cr_{0.7}O_3$ (L).

that diffuses inside, which can cause more Cr(III) to oxide to Cr(VI) (given the atmosphere in which the calcinations are conducted), as detected in the Cr(VI) analysis performed on the washing liquids and by the XPS measurements.

Taking into account the above mechanism, the results obtained with regard to coloration and segregation of Cr(VI) in the washing liquids might be explained in terms of the difference in particle sizes shown in Fig. 4, because though a greater uniformity is observed in industrial grade and CP grade Cr_2O_3 particle sizes, industrial grade Fe_2O_3 particle sizes exhibit a greater scatter. If reagent particle sizes are different (as is the case of industrial raw materials), end coloration uniformity will be poorer. Moreover, as there are Fe_2O_3 particles of different sizes, the quantity of Cr(III) that diffuses inwards will vary with respect to that which sublimes in the particles, possibly leading to sublimation of a greater quantity of chromium as Cr(VI) than when raw materials with a more uniform particle size are used, as is the case in CP grade raw materials. That is, a difference in particle sizes entails poorer quality black coloration though it reduces the quantity of segregated Cr(VI). Note that both cases lie within the accepted legal limit, as in European legislation the permitted quantities for Cr(VI) in water emissions are between 2 and 10 ppm.

Figs. 5 and 6 respectively show the Mössbauer spectra of the two samples $Fe_{1.3}Cr_{0.7}O_3$ (I) and $Fe_{1.3}Cr_{0.7}O_3$ (L) fired at 1200 °C/2 h. The spectra, which are very similar, are properly fitted with a distribution of sextets with hyperfine field ranging from 40 to 51 T. In both samples the isomer shifts (IS) and quadrupole splitting (QS) of the sextets in the distribution are respectively 0.35 mm s^{-1} and −0.28 mm s^{-1}, typical of Fe^{3+} and very close to the values expected for crystalline haematite[23] at room temperature (IS = 0.3 mm s^{-1}, QS = −0.197 mm s^{-1}).

For the two samples, the distribution shows that the most probable value of the hyperfine field is about 48 T and the mean hyperfine value is 47.3 T, which are values lower than that observed in pure α-Fe_2O_3 (51.75 T at 300 K). This indicates that the neighbouring of the Fe^{3+} sites has been altered with respect to that of α-Fe_2O_3. However, the changes mainly affect the hyperfine magnetic field and have little influence on the IS and QS, which are related to the electron density and electric field gradient at the nucleus of Fe^{3+} ions, respectively. Thus, this can be indicative of Cr^{3+} substitution at the Fe^{3+} sites (Cr is not magnetic, but is similar from the charge point of view).

However, it should be noted that the foregoing spectra could also be fitted to two sextets (each sextet would correspond to an Fe site) with hyperfine field values of 48.4 and 46.3 T which more closely approach those of Fe_3O_4 (49 and 46 T) in the composition prepared with industrial grade reagents than with CP grade reagents. However, the values

Table 4
O1s, Fe2p and Cr2p binding energies and surface atomic ratio for $Fe_{1.3}Cr_{0.7}O_3$ (I) and $Fe_{1.3}Cr_{0.7}O_3$ (L) fired at 1200 °C/2 h

Sample	(Vc[a]	Fe2p (eV)	Cr2p[b] (eV)	O1s[b] (eV)	Fe/O	Cr/O
$Fe_{1.3}Cr_{0.7}O_3$ (L)	11.7	710.4	576.0 (46655) 578.6 (12093)	529.6 (231600) 531.8 (88534)	0.205	0.191
$Fe_{1.3}Cr_{0.7}O_3$ (I)	8.45	710.4	576.6 (13803) 579.1 (2248)	530.0 (172600) 532.2 (64661)	0.250	0.200

[a] Charge correction related to the C1s peak.
[b] The peak area of each component is given in brackets.

of the isomer shift and the quadrupole shift do not fit those of Fe_3O_4 as well, which is why it is considered these could be assigned to Fe_3O_4 replaced with Cr.

The O1s, Fe2p and Cr2p binding energies recorded in the XPS spectra for $Fe_{1.3}Cr_{0.7}O_3$ (I) and $Fe_{1.3}Cr_{0.7}O_3$ (L) fired at 1200 °C/2 h are listed in Table 4, together with the surface atomic ratio.

The O1s core level line of the $Fe_{1.3}Cr_{0.7}O_3$ (I) sample shows the presence of two components at 530 and 532.25 eV. The peak at 532 eV can be related either to OH or carbonate impurities, while the O1s binding energy for both iron or chromium oxide is approximately 530 eV. The O1s core line of the $Fe_{1.3}Cr_{0.7}O_3$ (L) sample shows a 0.4 eV shift to lower binding energy, which could probably be related to some charge effects.

The Cr2p core level XPS spectra of both $Fe_{1.3}Cr_{0.7}O_3$ (I) and $Fe_{1.3}Cr_{0.7}O_3$ (L) samples are presented in Fig. 7. In both cases a slight asymmetry in the high binding energy region of the Cr2p3/2 line is observed, leading to a two components decomposition of the Cr2p core line. Binding energies of 576.6 and 579.15 eV are obtained for the $Fe_{1.3}Cr_{0.7}O_3$ (I) sample, while a ~0.5 eV shift to lower binding energy is observed for the $Fe_{1.3}Cr_{0.7}O_3$ (L) sample. This shift is the same as observed in the O1s core level line, probably related to charge effects. Thus, we can assume the same type of chromium species in both samples. According to literature data, the 576.6 eV component, which is the predominant one in both samples, can be related to the Cr(III) species, while the 579.6 eV component is related to the Cr(VI)[24] or Cr(V) species[25]. The presence of the more oxidised Cr species is low in both samples (20% in the $Fe_{1.3}Cr_{0.7}O_3$ (L) sample, and 14% in the $Fe_{1.3}Cr_{0.7}O_3$ (I) sample).

The Fe2p core level XPS spectra are shown in Fig. 8 for both $Fe_{1.3}Cr_{0.7}O_3$ (I) and $Fe_{1.3}Cr_{0.7}O_3$ (L) samples. In both cases, the peak is rather asymmetric. Similar asymmetry has been observed in the literature, due to multiplet splitting. The binding energy of the Fe2p3/2 peak in the $Fe_{1.3}Cr_{0.7}O_3$ (I) sample is 710.4 eV, which can be related to Fe_3O_4,[26] containing both Fe(III) and Fe (II) species.

In the $Fe_{1.3}Cr_{0.7}O_3$ (L) sample, a peak at a binding energy of 710.4 eV is observed, together with a more pronounced shake-up satellite at 719.0 eV. The presence of this satellite is characteristic of Fe(III). Note that in the $Fe_{1.3}Cr_{0.7}O_3$ (I) sample, this satellite structure is not clear at all, confirming the coexistence of both Fe(III) and Fe(II) species. Further note a shift of 0.4 eV to a lower binding energy observed in the $Fe_{1.3}Cr_{0.7}O_3$ (L) sample due to charge effects. Thus the "corrected" binding energy of the Fe2p3/2 core line should be 710.8 eV, close to the value reported for Fe(III).[26,27]

In accordance with the XPS spectra, no differences are observed in the oxygen and chromium species, while a small difference in the oxidation state of the iron species can be inferred between the $Fe_{1.3}Cr_{0.7}O_3$ (I) and $Fe_{1.3}Cr_{0.7}O_3$ (L) samples. The Fe(III) species seems to be the only one in

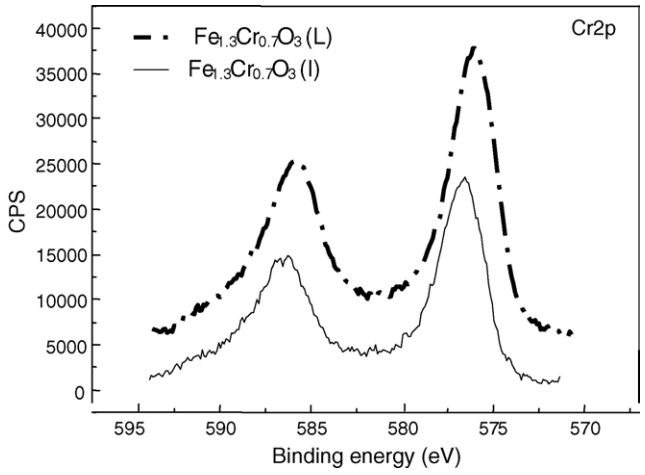

Fig. 7. Cr2p core level XPS spectra of samples $Fe_{1.3}Cr_{0.7}O_3$ (I) and $Fe_{1.3}Cr_{0.7}O_3$ (L).

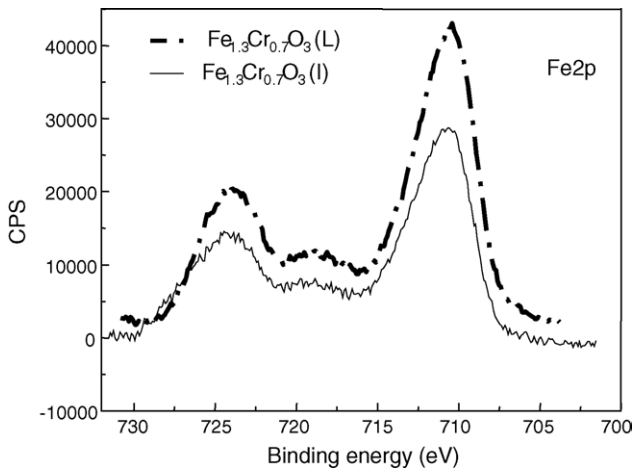

Fig. 8. Fe2p core level XPS spectra of samples $Fe_{1.3}Cr_{0.7}O_3$ (I) and $Fe_{1.3}Cr_{0.7}O_3$ (L).

the $Fe_{1.3}Cr_{0.7}O_3$ (L) sample, while both Fe(II) and Fe(III) can be inferred in the $Fe_{1.3}Cr_{0.7}O_3$ (I) sample. This is confirmed by the auger parameter. Indeed, the same auger parameter has been obtained for Cr ($\alpha = 1088.2$ eV) while the Fe auger parameter is 1.45 eV higher in the $Fe_{1.3}Cr_{0.7}O_3$ (L) sample ($\alpha = 1414.6$ eV) than in the $Fe_{1.3}Cr_{0.7}O_3$ (I) sample ($\alpha = 1413.15$ eV). Note that the auger parameter is independent of charge effects and depends only on coordination, oxidation state and environment of the metal. Thus, differences in the nature of the iron species can be inferred according to the XPS and X-ray induced AES spectra, while the nature of the chromium species seems to be similar in both samples.

According to the XPS data, in the pigment synthesised with industrial grade raw materials, Fe is found in oxidation states +2 and +3 as Fe_3O_4. As the Mössbauer data are also consistent with the existence of Fe_3O_4 replaced with chromium, the formation of an $Fe^{II}(Fe^{III},Cr^{III})_2O_4$ brown spinel can be assumed. The Mössbauer and XPS data would both explain the differences remarked previously in the values of the chromatic coordinates and of the Cr(VI) content in the washing liquids. The greater quantity of Fe(II) detected in the sample prepared with industrial grade reagents might stem from the presence of sulphur as an impurity, determined by XRF analysis (Table 1), which could reduce Fe(III).

4. Conclusions

- The best composition and synthesising conditions for obtaining a black ceramic pigment have been established without the use of a more complicated mixture of different oxides, as is the case of a black pigment used in the ceramic industry.
- The use of industrial grade reagents enables obtaining a black ceramic pigment with a low environmental impact, though with poorer chromatic quality when compared with a sample prepared under the same conditions but made with reagents of greater purity.
- The differences in behaviour of samples prepared with industrial quality and CP grade reagents are to be attributed to both the presence of Fe(II) and differences in particle sizes.
- The presence of Fe(II) in industrial quality reagents detected mainly by XPS measurements allows an $Fe^{II}(Fe^{III},Cr^{III})_2O_4$ brown spinel to form, which could explain the differences in the chromatic coordinates.

Acknowledgements

The research was supported by Ministerio de Ciencia y Tecnología project MAT 2002-02099 and by Fundació Caixa Castelló-Universitat Jaume project P1-1B2003-27. Grateful thanks to Africa Garcia for her invaluable help.

References

1. Buxbaum, Gunter, ed., *Industrial Inorganic Pigments*. 2nd ed. Wiley-VCH, New York, 1998.
2. Duffus, J. H., © 2002 IUPAC. *Pure Appl. Chem.*, 2002, **74**(5), 793.
3. Eppler, R. A. and Eppler, D. R., *Glazes and Glass Coatings*. American Ceramic Society, Westerville, OH, 2000.
4. Eppler, R. A., *Ceram. Bull.*, 1980, 562.
5. Eppler, R., Ulmann's encyclopedia of science and technology. *Ceram. Colorants*, 1986, **A5**, 545–556.
6. US Patent 4, 205,996, 1980.
7. Chronister, S. A. and Chen, W., *Am. Ceram. Soc. Bull.*, 1994, **73**(9), 71.
8. Airey, A. C. and Roberts, W., *Ceram. Eng. Sci. Proc.*, 1987, **8**(11–12), 1168.
9. Cordoncillo, E., Del Rio, F., Carda, J. B., Llusar, M. and Escribano, P., *J. Eur. Ceram. Soc.*, 1998, **18**, 1115.
10. http://www.oni.escuelas.edu.ar/olimpi2000/cap-fed/elagua/impacto/medio/amec.htm.
11. http://www.epa.gov/tio/products/newsltrs/gwc/gwchexa.htm.
12. http://www.ecoportal.com.ar/articulos/lastoscas.htm.
13. See: http://www.ecoweb-la.com/notas/rpe/ga1443.htm.
14. Puxbaum, H., In *Metals and Their Compounds in the Environment*, ed. E. Merian. VCH, Weinheim, 1991.
15. DCMA, Classification and chemical description of the mixed metal oxide inorganic coloured pigments. *Metal Oxides and Ceramics Colours Subcommittee* (*2nd ed.*). Dry Colour Manufacturer's Association, Washington DC, 1982.
16. Muan, A. and Sōmiya, S., *J. Am. Ceram. Soc.*, 1960, **43**(4), 207.
17. Escribano, P., Carda, J. B. and Cordoncillo, E., *Esmaltes y Pigmentos Cerámicos, Enciclopedia Cerámica* (*3er Tomo, ed.*). Faenza Editrice Ibérica, 2001.
18. Dilabert, E. J., *Medida del color*. Servicio de Publicaciones, Madrid, Spain, 1982.
19. *Methods for Chemical Analysis of Water and Wastes*, EPA-600/4-82-055, December 1982. Methods 218.4 and 218.5.
20. Wagner, C. D., Davis, L. E., Zeller, M. V., Taylor, T. A., Raymond, R. H. and Gale, L. H., *Surf. Interface Anal.*, 1981, **3**(5), 21.
21. Shannon, R. D. and Prewitt, C. T., *Acta Crystallogr., Sect. A*, 1976, **32**, 751.
22. Escardino, A., Barba, A. and Mestre, S., *Mass Charge Transport Inorg. Mater.*, 2000, 627.
23. Greenwood, N. N. and Gibb, T. C., *Mössbauer Spectroscopy*. Chapman and Hall, London, 1971, p. 241 (chapter 10).
24. (a) Allen, G. C., Curtis, M. T., Hooper, A. J. and Tucker, P. H., *J. Chem. Soc. Dalton Trans.*, 1973, 1675;
(b) Cimino, A., De Angelis, B. A. *et al.*, *J. Catal.*, 1976, **45**, 316.
25. Gazzoli, D., Ochiuzzi, M., Cimino, A., Minelli, G. and Valigi, M., *Surf. Interface Anal.*, 1992, **18**, 315.
26. Allen, G. C., Harris, S. J. and Jutson, J. A., *Appl. Surf. Sci.*, 1989, **37**, 111.
27. Kuivila, C. S., Butt, J. B. and Stair, P. C., *Appl. Surf. Sci.*, 1988, **32**, 99.